nature neuroscience

ARTICLES

Pore region of TRPV3 ion channel is specifically required for heat activation

Jörg Grandl[1,3], Hongzhen Hu[2,3], Michael Bandell[2], Badry Bursulaya[2], Manuela Schmidt[1], Matt Petrus[2] & Ardem Patapoutian[1,2]

Ion channels can be activated (gated) by a variety of stimuli, including chemicals, voltage, mechanical force or temperature. Although molecular mechanisms of ion channel gating by chemical and voltage stimuli are understood in principal, the mechanisms of temperature activation remain unknown. The transient receptor potential channel TRPV3 is a nonselective cation channel that is activated by warm temperatures and sensory chemicals such as camphor. Here we screened ~14,000 random mutant clones of mouse TRPV3 and identified five single point mutations that specifically abolish heat activation but do not perturb chemical activation or voltage modulation. Notably, all five mutations are located in the putative sixth transmembrane helix and the adjacent extracellular loop in the pore region of mouse TRPV3. Although distinct in sequence, we found that the corresponding loop of frog TRPV3 is also specifically required for heat activation. These findings demonstrate that the temperature sensitivity of TRPV3 is separable from all other known activation mechanisms and implicate a specific region in temperature sensing.

Temperature sensing is critical for living organisms to interact with their environment. Sensory neurons in dorsal root and trigeminal ganglia detect changes in temperature and signal to the spinal cord and the brain[1]. Recently, several transient receptor potential (TRP) ion channels have been identified as being receptors of physiological temperature, and gene ablation studies have revealed a requirement for these thermoTRPs in innocuous and noxious thermosensation[1,2]. At least six thermoTRPs have been identified that are activated by temperature and are expressed in skin and/or sensory neurons. TRPV1 (approximate threshold 43 °C), TRPV2 (52 °C), TRPV3 (33 °C) and TRPV4 (25–34 °C) are activated by heating[3–9], and TRPM8 (25 °C) and TRPA1 (17 °C) are activated by cooling[10–13]. TRPV3 has been shown to be expressed in mouse skin keratinocytes and human sensory neurons of dorsal root ganglia, and TRPV3 knockout mice show impaired responses to innocuous and noxious heat[5,8,14]. Similar to other TRP channels, TRPV3 is a polymodal receptor that is also activated by chemical ligands such as the natural compound camphor and the synthetic compound 2-aminoethoxydiphenyl borate (2APB)[15–17].

Most TRP channels are tetrameric calcium-permeable nonselective cation channels with six transmembrane domains and an ion pore between transmembrane domains 5 and 6 (TM5 and TM6, respectively)[18,19]. Several domains/residues have been mapped in thermo TRPs that are required for chemical and voltage-dependent activation. However, the mechanism for temperature activation remains unsettled. Temperature activation of most thermoTRPs is retained in cell-free membranes, arguing that the mechanism is independent of cytoplasmic processes[20]. Voltage-dependent gating has been proposed as a basic principle for temperature sensing in heat-activated TRPV1 and cold-activated TRPM8 channels[21–23]. In this theory, temperature and chemical compounds shift the voltage-dependent activation curves of TRPV1 and TRPM8 toward physiological membrane potentials. Recently, it has been proposed that voltage, temperature and chemical cues act through independent mechanisms, but interact allosterically with each other[24–26]. Chimeras with swapped C-terminal domains between TRPM8 and TRPV1 have switched temperature phenotypes, suggesting that the C-terminal domains of thermoTRPs might determine the directionality of the temperature response[27,28].

Little is known about the temperature activation underlying other thermoTRPs, including TRPV3. Many ion channels appear to be modular proteins with specific structural domains that are required for sensing individual stimuli. For example, charged residues in specific domains render channels voltage sensitive. We thus hypothesized that TRPV3 might possess residues or domains that specifically affect temperature activation without changing overall channel function and set out to identify them.

RESULTS

Random mutagenesis screen

To find residues in TRPV3 that are required for heat activation, we constructed a mutant library of ~14,000 clones of mouse TRPV3, each containing, on average, 2.5 randomly introduced single-point mutations[29]. In a 384-well format, we screened human embryonic kidney (HEK) cells that were transiently transfected with DNA from these clones using a calcium-influx assay with a fluorescent imaging plate

[1]Department of Cell Biology, The Scripps Research Institute, La Jolla, California 92037, USA. [2]Genomics Institute of the Novartis Research Foundation, San Diego, California 92121, USA. [3]These authors contributed equally to this work. Correspondence should be addressed to A.P. (apatapou@gnf.org).

Received 7 April; accepted 24 June; published online 10 August 2008; doi:10.1038/nn.2169

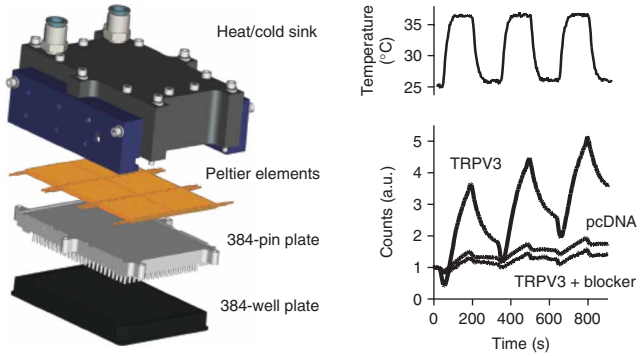

Figure 1 TRPV3 mutant library screen. Image of custom-designed device that was used to control temperature across 384-well plates during optical readout in a FLIPR. Peltier elements (orange) chilled by a water chamber from the top (dark gray and blue) heat or cool a metal plate on the bottom (light gray) with single pins penetrating into a 384-well plate (black). Right, the activation profile of TRPV3 upon temperature stimulation (above) and its block by 10 μM ruthenium red and pcDNA-transfected cells is shown.

reader (FLIPR). A custom-designed device was used to rapidly and precisely change the temperature across a 384-well plate simultaneous with optical readout, enabling us to measure compound and heat activation of TRPV3 clones in a high-throughput manner (**Fig. 1** and **Supplementary Fig. 1** online).

Using temperature, 2APB and camphor as agonists, we identified, validated and sequenced 15 clones from this library that showed normal 2APB and camphor dose-response curves, but had strongly reduced heat responses compared with wild-type TRPV3 (**Supplementary Table 1** online). Because most of the clones (12 of 15) had a point mutation in the proximity of either TM1 or TM6, we decided to engineer each of these mutations individually. Again, we measured full dose-response curves for activation by 2APB, camphor and temperature. Of the 12 single-point mutations tested, only five (Asn643Ser, Ile644Ser, Asn647Tyr, Leu657Ile and Tyr661Cys) specifically affected heat activation without affecting activation by 2APB or camphor (**Fig. 2**). Notably, all five were clustered in a small domain adjacent to the channel pore (see below).

Electrophysiology on selected mutants

To validate our temperature screening method, we carried out patch-clamp experiments on HEK cells that were transiently transfected with DNA for three randomly selected single-point mutants (Ile644Ser, Asn647Tyr and Tyr661Cys) that showed complete and specific loss of temperature activation. Three sequential heat ramps followed by a pulse of 30 μM 2APB confirmed that the heat response in these mutants was indistinguishable from that of pcDNA-transfected cells, whereas wild-type TRPV3 responses are large and sensitized by consecutives stimulations, as reported previously[30] (**Fig. 3**).

Because the identified mutations are located in the pore region, we carried out single-channel and whole-cell recordings, which demonstrated that the 2APB-dependent unitary conductance and the ion selectivity of TRPV3 were unaltered by these mutations (**Fig. 4a**,**b**). In addition, we observed that these mutants have two distinct current-voltage phases during prolonged activation, a feature that has been described previously for wild-type TRPV3 (**Fig. 4c**,**d**)[31]. Although mutation of tyrosine 661 to cysteine (Tyr661Cys) seemed to slow the entry of the channel into phase 2, altogether these data demonstrate that these three point mutations do not alter the basic properties of TRPV3.

Voltage is a known modulator of TRPV3 activation and we investigated the voltage dependence for each mutant by a voltage-step protocol. From steady-state currents, we calculated the voltage causing half-maximal activation (V_{half}) and found that it was identical to wild-type TRPV3 (**Fig. 4e–h**). Hence, these three mutations uncouple heat from chemical and voltage sensitivity.

Detailed mutagenesis of a heat-specific domain

Our high-throughput random mutagenesis screen is not expected to be at saturation, as the library will not come close to carrying mutations in each amino acid with substitutions representing all of the other 19 residues. To explore the temperature-sensitive domain of TRPV3 in

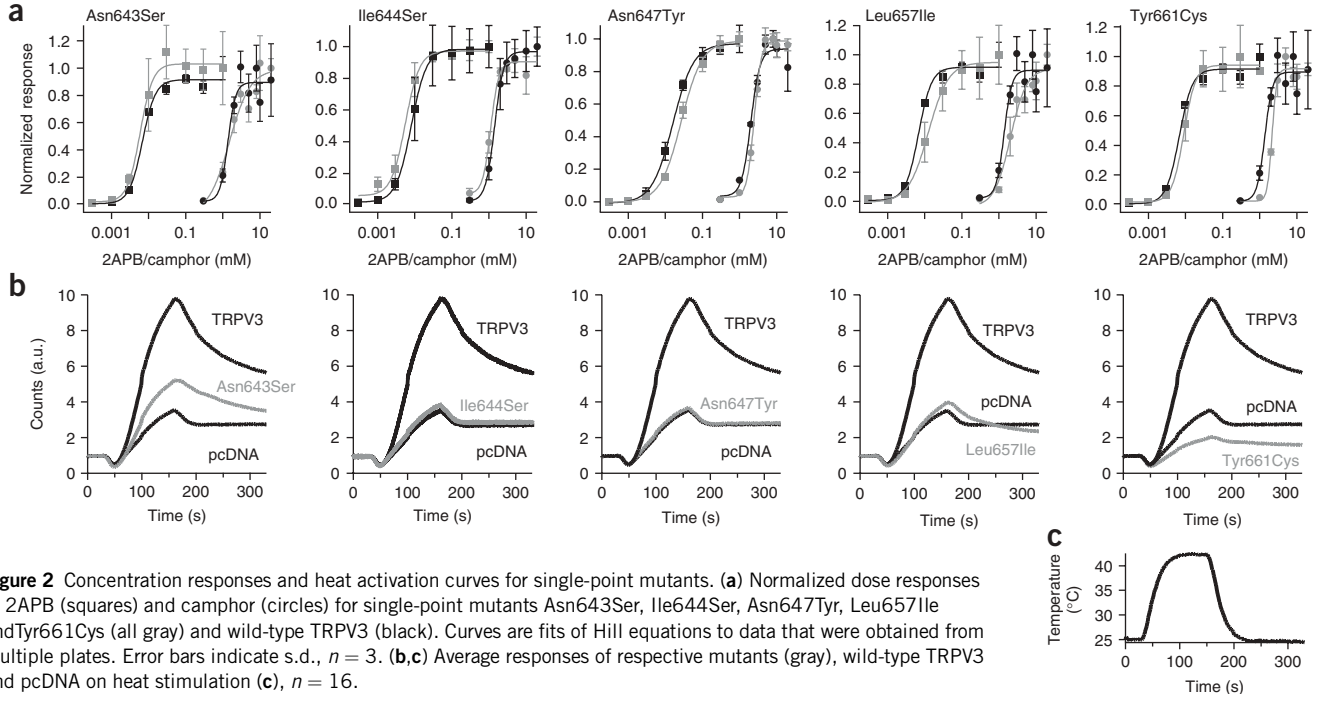

Figure 2 Concentration responses and heat activation curves for single-point mutants. (**a**) Normalized dose responses of 2APB (squares) and camphor (circles) for single-point mutants Asn643Ser, Ile644Ser, Asn647Tyr, Leu657Ile andTyr661Cys (all gray) and wild-type TRPV3 (black). Curves are fits of Hill equations to data that were obtained from multiple plates. Error bars indicate s.d., $n = 3$. (**b**,**c**) Average responses of respective mutants (gray), wild-type TRPV3 and pcDNA on heat stimulation (**c**), $n = 16$.

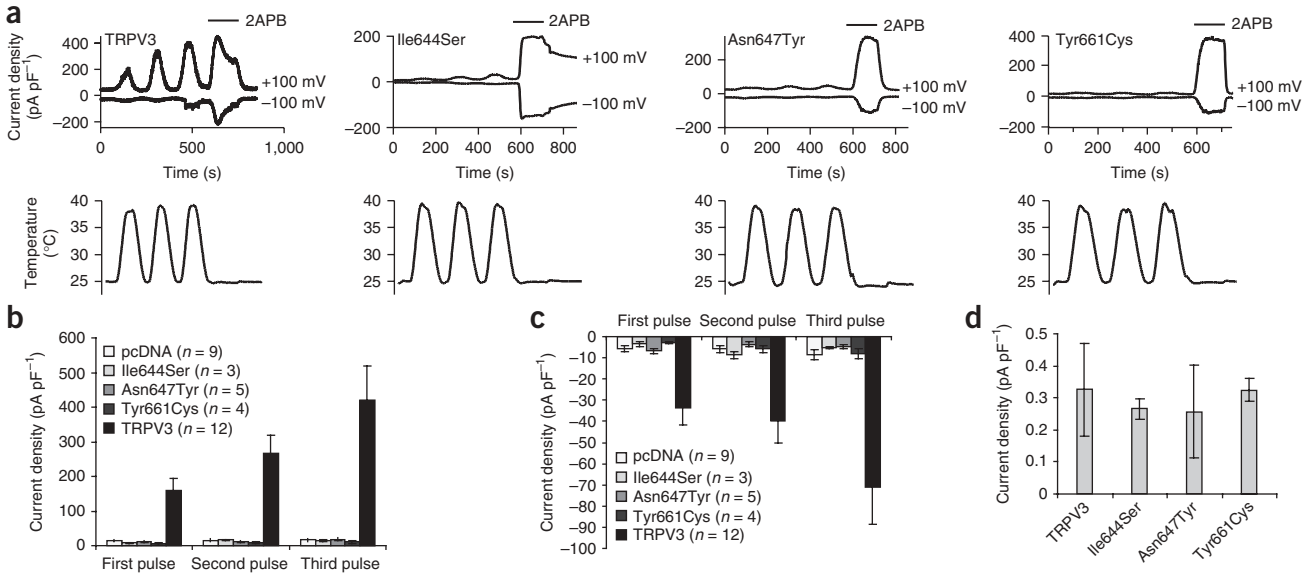

Figure 3 Electrophysiology of heat sensitivity of single-point mutants Ile644Ser, Asn647Tyr, Tyr661Cys and wild-type TRPV3. (**a**) An example of current-density traces from whole-cell recordings from transiently transfected HEK293 cells at +100 mV and −100 mV. Cells were stimulated with three consecutive heat ramps (below) and were subsequently challenged with 30 μM 2APB to determine channel expression. (**b**,**c**) Averaged maximal current densities for each heat pulse at +100 mV (**b**) and −100 mV (**c**). Error bars are s.e.m. Numbers (*n*) of individually tested cells are indicated. (**d**) Average current densities evoked by 30 μM 2APB without prior heat stimulation. Error bars indicate s.d., $n = 3$.

more detail, we generated a mutant library containing 45 random point mutations for each position between the selectivity filter and the last position that was identified in our initial screen (Leu642–Thr660) and tested it with temperature, 2APB and camphor (**Supplementary Fig. 2** online). We found temperature-specific mutations in three additional positions (**Supplementary Table 2** online), further highlighting the importance of this domain for temperature sensitivity (**Fig. 5a**). Notably, mutations in TM6 were located in a periodic pattern, potentially aligned on one side of an α-helical structure. Modeling the TRPV3 pore on the basis of the crystal structure of Kv1.2 (ref. 32) suggested that the three mutations are exposed to the lipid-facing side of TM6 (**Fig. 5b–e**).

Xenopus TRPV3 and TRPV chimeras

TRPV3 sequence orthologs can be found in tetrapods, but not in bony fishes or invertebrates. The most distant ortholog of mammalian TRPV3 with sequence information is that of *Xenopus tropicalis* (53% identity with mouse TRPV3). The extracellular loop region in question is highly divergent from mouse sequences, with all six amino acids following the predicted selectivity filter (E638–P643) being different in mouse and frog (**Fig. 6a**). This led us to speculate that frog TRPV3 would be heat insensitive. To our surprise, we found that frog TRPV3 responded to heat and 2APB. Although these data suggest that frog TRPV3 is heat gated, it should be noted that we added small N- and C-terminal mouse sequences to obtain a functional channel (see Methods). To determine directly whether extracellular loop residues of frog TRPV3 are involved in temperature activation, we generated randomized single-point mutants for the six divergent positions and measured their sensitivity to heat and 2APB. Notably, we discovered heat-specific hits at every residue (**Fig. 6b**,**c** and **Supplementary Table 3** online), demonstrating that this region, although highly different in primary sequence, is required for temperature activation.

In addition to TRPV3, several other TRPV channels are activated by heat (TRPV1 and TRPV4 and rat TRPV2), whereas others are not (human TRPV2 and mouse TRPV6)[1,9]. When aligning the amino-acid sequences of these channels, we noticed that functional regions such as the pore, transmembrane domains and selectivity filter were all well conserved, but the loop region that contains many of the discovered heat-specific mutations varied largely (**Supplementary Fig. 3** online). We therefore engineered chimeric channels, in which we placed different domains into a TRPV3 background and vice versa, and tested their heat sensitivity and response to their respective ligands (**Supplementary Fig. 3**). As expected, our stringent requirement that chimeras have wild type–like responses to chemical stimulation to draw conclusions about the nature of heat sensitivity was not fulfilled by most constructs (**Supplementary Table 4** online). However, the exchange of a short domain of the heat-insensitive channel human TRPV2 into the background of mouse TRPV3 was sufficient to completely abolish heat activation, but did not affect 2APB and camphor sensitivity (**Fig. 6d**,**e**). A similar chimera between rat TRPV2 (which is heat activated) and mouse TRPV3 showed no heat responses, but also caused a large shift in chemical responses, making it difficult to draw any conclusions from this chimera (**Supplementary Fig. 3** and **Supplementary Table 4**). Therefore, although these chimeras do not make predictions of TRPV2 heat sensitivity, they underline the necessity of this region for heat sensitivity in TRPV3.

DISCUSSION

Categorized by their mechanism of gating, ion channels can be activated by signals such as specific ligands, voltage or mechanical force. To date, the mechanisms underlying thermal activation of TRP channels represent a fundamental unknown in the field. The identification of structural elements in the channel that are involved in temperature sensing would be a first step toward a molecular and biophysical understanding of temperature gating. Our central finding in this study is the discovery of several single-point mutations that are clustered in a small domain in the pore region and TM6 that uncouple heat activation of TRPV3 from all other known activation mechanisms.

Isolating temperature mutations with normal camphor and 2APB responses ensured that the selected mutant channels were viable and

basic properties, such as expression level and overall functionality of TRPV3, were not perturbed. Furthermore, this approach directly addresses the question of whether activation of this channel by chemicals and heat can be separable. The fact that we have identified point mutants that are normal in all aspects of TRPV3 modulation (**Figs. 3** and **4**) except for heat responses strongly suggests that at least part of the heat activation process is unique. This does not imply that chemical activation and heat activation are completely separable. Indeed, there is ample evidence that thermoTRPs are allosterically gated polymodal receptors[25].

Two important aspects of ion channel functionality are the abilities of the proteins to sense stimuli and to gate (open) the channel pore. For example, TRP-related six transmembrane-containing voltage-activated ion channels sense voltage through positively charged amino acids in TM4. The movement of this domain is thought to transduce a conformational change on nearby pore-spanning TM6 and directly gate the ion channel. Is there a similar temperature sensor domain in thermoTRPs? Is this domain localized or is it scattered throughout the protein? It is very notable that all of the heat-specific mutations that we identified are clustered in the pore region.

We found that a TRPV3 chimera carrying 28 amino acids of TRPV2 (TM6 and loop region) has normal chemical activation, but has no heat activation. This result further reinforces the conclusion that the TM6 and adjoining extracellular loop domain are specifically required for

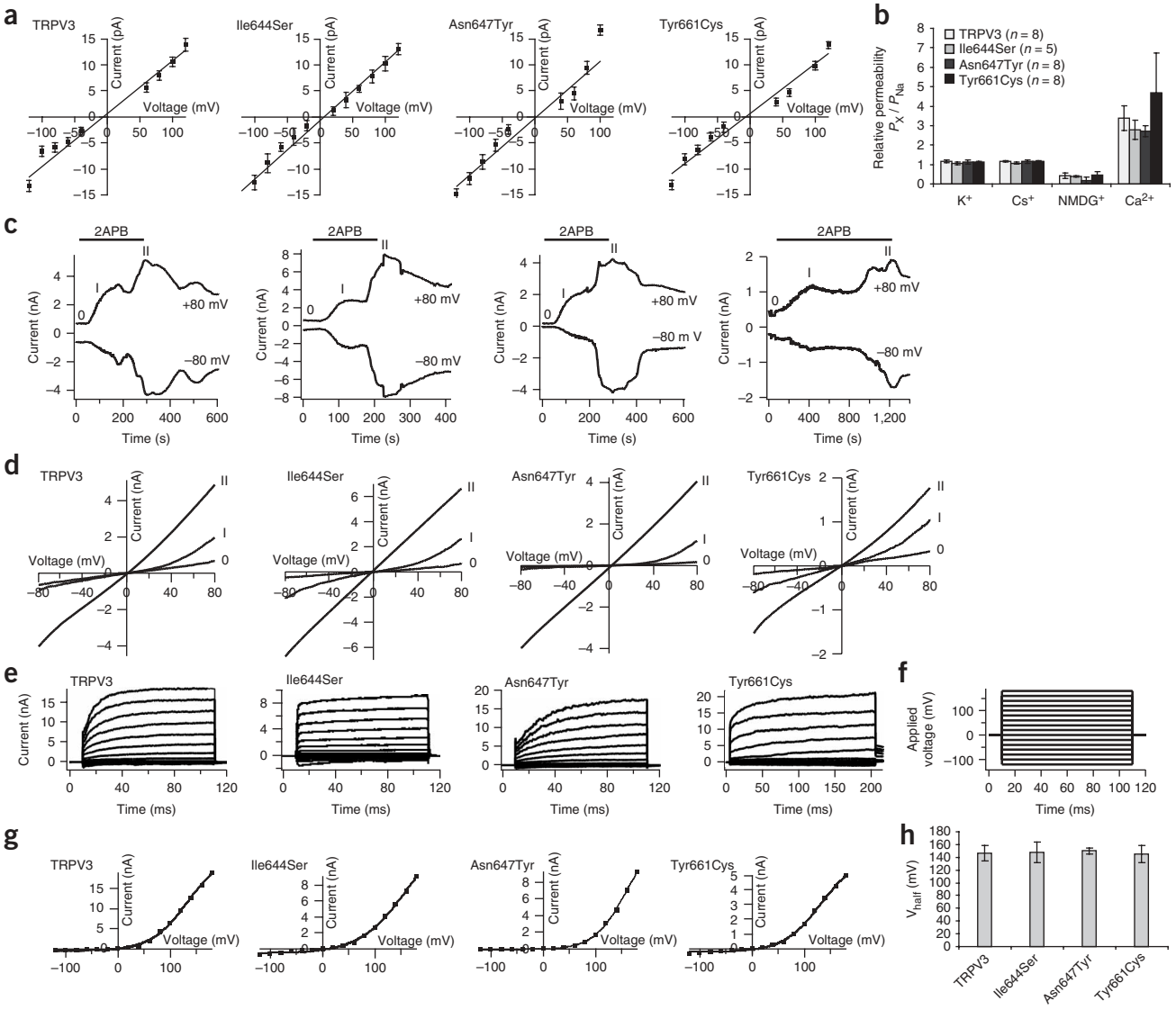

Figure 4 Basic channel properties of Ile644Ser, Asn647Tyr, Tyr661Cys and wild-type TRPV3. (**a**) Single-channel current amplitudes obtained from Gaussian fit to current histograms as a function of voltage. Error bars are s.d., straight lines indicate linear fits to the data. The average values ± s.d. of unitary conductance were 112 ± 4 pS (Ile644Ser), 109 ± 6 pS (Asn647Tyr), 96 ± 6 pS (Tyr661Cys) and 101 ± 5 pS (wild-type TRPV3). (**b**) Calculated relative permeabilities of TRPV3 and mutant channels for selected ions. Numbers (*n*) are indicated for each channel, error bars are s.d. (**c**,**d**) Examples of whole-cell currents ($n = 3$) from cells transfected with TRPV3 or mutant channels, continuously stimulated by 25 μM 2APB, at –80 mV and +80 mV. Respective current-voltage measurements before (0) and during (phase I and phase II) stimulation are shown in **d**. Note that mutant Tyr661Cys entered phase II only after prolonged application of 2APB as compared with wild-type TRPV3. (**e**–**g**) Examples of current recordings from whole-cell patches, stimulated by 30 μM 2APB during a voltage-step protocol (**f**), and respective current-voltage plots from steady-state currents (**g**). Lines show sigmoid fits to the data points. Note that mutant Ile644Ser had a faster voltage-activation than wild-type TRPV3. (**h**) Average values ± s.d. ($n = 3$) of voltage that caused half-maximal steady-state currents (V_{half}).

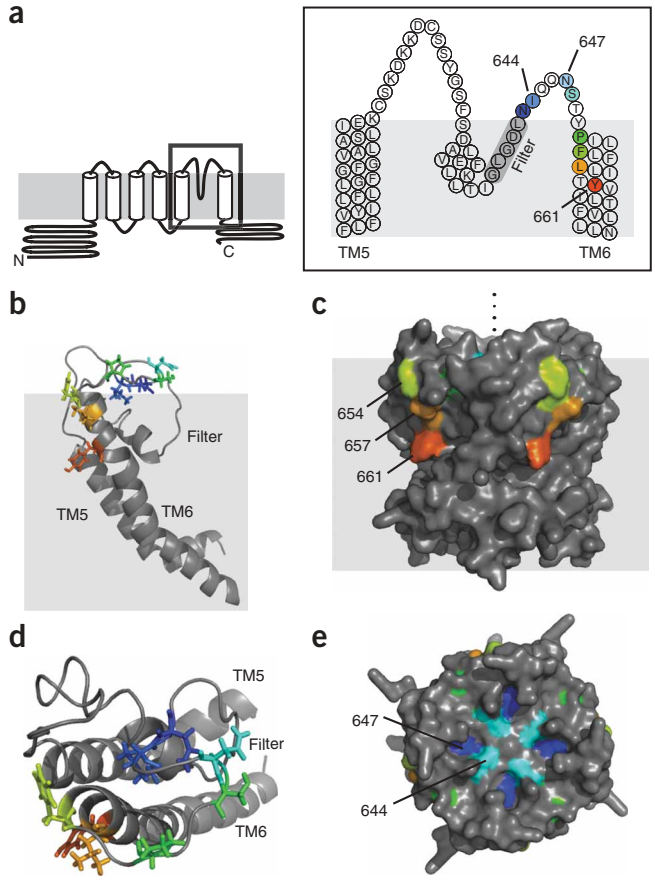

Figure 5 Location of the heat-sensitive domain. (**a**) A schematic of the TRPV3 channel topology with the positions of heat-specific mutations indicated in color is shown. Residues contributing to the selectivity filter are highlighted in gray. (**b**) Side view of homology model structure of the pore region of one subunit. The side chains of heat-specific mutations are colored individually. (**c**) Side view of the predicted surface of the TRPV3 pore region homology model. Temperature-specific mutations (Phe654Ser, Leu657Glu and Tyr661Cys) line the putative membrane exposed part of TM6 and are colored individually. (**d**) Top view of the homology model structure of the pore region of one subunit. (**e**) Top view of the predicted surface of the TRPV3 pore region homology model.

the heat sensitivity of TRPV3. Our data do not reveal specifically how these mutations affect temperature activation mechanistically. Mutations could shift the activation threshold to temperatures that are higher than the ones that we tested (no responses up to 50 °C, data not shown) or completely disrupt the temperature-sensing mechanism. Activation of the three well-characterized mutants by 2APB at 40 °C (data not shown) indicates that these channels remain functional at high temperatures. Our electrophysiological data indicate that point mutations have a slight effect on gating kinetics in some cases, but leave the overall gating equilibrium unchanged, and detailed dwell-time analysis might provide a more mechanistic insight. In either case, these results suggest that TM6 and the adjacent extracellular loop are essential for temperature sensing or for the gating transition from an upstream temperature-sensing domain. The close proximity of this temperature module to the pore makes it tempting to speculate that temperature-induced conformational changes in this extracellular loop and adjoining TM6 helix may directly gate the channel. In closely related TRPV1, the pore loop is known to be an activation domain for protons and other cations, suggesting that this domain might serve different sensory functions[33,34]. Finally, a recent report found the pore helix of TRPVs to be crucial for determining the overall gating equilibrium of these channels by various agonists, raising the possibility that the TM6 domain that we identified could directly interact with the pore helix to gate the channel[35].

Our studies have focused on TRPV3 and it may be that the mechanism of temperature sensitivity in other thermoTRPs is different[20,25]. However, it is also possible that the TM6 region identified here for TRPV3 and the C-terminal domain identified in TRPV1 and TRPM8 (which is mainly involved in determining the directionality of temperature gating) might work in concert[28]. The temperature domain that we isolated for mouse TRPV3 appears to be conserved in *Xenopus* TRPV3, although the primary sequence of the loop region is not conserved between the two species. Perhaps biophysical characteristics of the loop region, such as conformation or flexibility, determine the requirement for heat sensitivity. Modeling of the TRPV3 pore suggests that the TM6

Figure 6 *Xenopus* TRPV3 and TRPV chimeric channels. (**a**) Alignment of the amino-acid sequences of mouse TRPV3, the chimeric construct hV2mV3-II and *Xenopus* TRPV3 from the pore region to TM6. The locations of different functional domains are indicated by gray boxes above the alignment. The locations of heat-specific single-point mutations are highlighted. The light gray box marks the swapped domain of the chimeric construct. (**b**) Average FLIPR responses of *Xenopus* TRPV3 and pcDNA ($n = 64$ each) and one of the heat-specific mutants, xTRPV3 D640L ($n = 4$), on heat-stimulation (below). (**c**) Average FLIPR response of *Xenopus* TRPV3 ($n = 64$), pcDNA ($n = 12$) and mutant D640L ($n = 4$) on stimulation with 25 μM 2APB. Error bars indicate s.d. (**d**) Average FLIPR responses of the chimera hV2mV3-II, TRPV3 wild type and pcDNA on heat stimulation (below) ($n = 48$). (**e**) Normalized FLIPR dose response for chimera hV2mV3-II and wild-type TRPV3 for 2APB (squares) and camphor (circles). Lines are fits of Hill equations to the data. Error bars indicate s.d., $n = 3$.

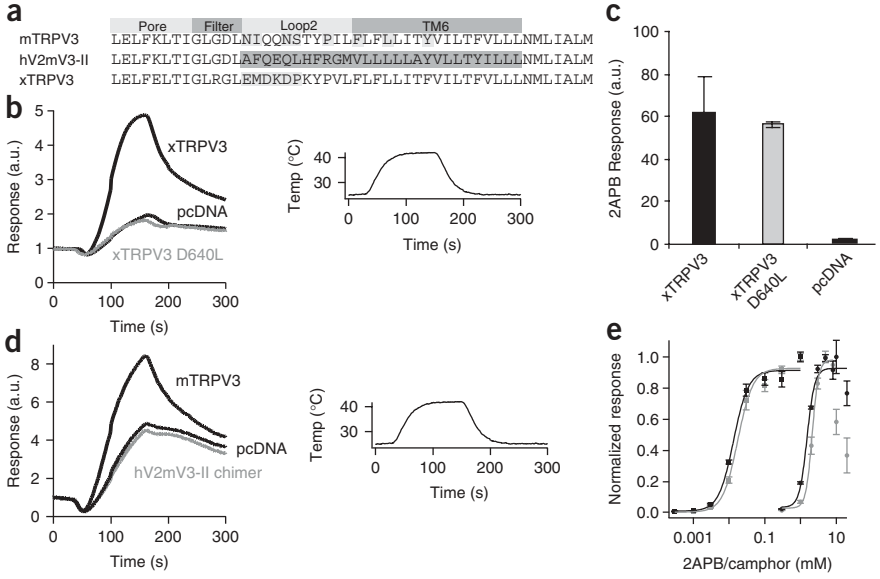

mutations are facing the membrane and puts forward an alternative hypothesis that protein-lipid interactions might be involved in temperature sensitivity. Future experiments can test these possibilities. For example, environmentally sensitive labels could probe stimulus-dependent structural rearrangements of this region. Recordings in artificial membranes could test whether heat activation of TRPV3 is dependent on the bilayer composition or structure. Finally, because temperature is equivalent to molecular motion, NMR experiments could be a promising approach for elucidating the mechanisms of temperature activation.

METHODS

Mutant library. Our methods for generating a random mutant library and for carrying out high-throughput screening for TRPV3 mutants are essentially the same as those described previously[29]. Error-prone PCR (Diversify PCR random mutagenesis kit, Clontech) was performed on the cloned mouse *Trpv3* gene, and we subsequently cloned the PCR product into the pcDNA5-FRT mammalian expression vector. Our previous studies found that the rate of mutation is approximately 5–6 base changes per clone (~4 amino-acid substitutions), which led to a high occurrence (~75%) of inactive mutants[1]. To decrease the rate of mutation, we digested the PCR product using a unique AvrII site, thereby generating two fragments, ~1.6 and 0.9 kb in size, which represented the two halves of the gene. We then cloned each fragment into a pcDNA5 vector containing the wild-type *Trpv3* gene, from which the corresponding fragment had been cut. Therefore, three mutant libraries, including the full-length and N- and C-terminal halves of mouse TRPV3, were generated. Sequence analysis of ten randomly picked clones confirmed that the total number of mutations per clone was ~2 amino acid changes. About 5,000 transformants from each library were picked and grown in 96-well plates containing 1.5 ml of terrific broth growth media per well. Plasmid DNA was isolated using 96-well plasmid miniprep consumables. DNA concentration was quantified and normalized to 40 ng μl^{-1} using a 96-well ultraviolet spectrophotometer and an automated pipetting station (MWG Biotech).

Cell culture and transfection. Using a Hewlett Packard Minitrak devise, we plated DNA in quadruplicate into poly-D-lysine–coated 384-well clear-bottom assay plates (Greiner) at 75 ng per well. Positive (wild-type TRPV3) and negative (mock transfection) assay controls were included. Transfections were carried out by adding Fugene 6.0 (0.2 µl per well, Roche) diluted in OPTI-MEM (Invitrogen) and trypsinized HEK293T cells (8,000 cells per well) to all wells. Transfected HEK293 cells were grown at 37 °C, 5% CO_2, in DMEM containing 4.5 mg ml^{-1} glucose, 10% heat-inactivated fetal bovine serum (vol/vol), 50 units ml^{-1} penicillin and 50 µg ml^{-1} streptomycin. Cells were washed with HANKS buffer by an Embla plate-washer (Molecular Devices) 2 d after transfection, loaded with the calcium-sensitive fluorophore Fluo3 (Molecular Devices) for 1.5 h, washed again and transferred to a FLIPR (Molecular Devices) to monitor fluorescence.

Temperature-altering device. The device for altering temperature consisted of six thermoelectric modules (HP199-1.4-0.8P, TeTechnology) that were in contact with an aluminum plate with 384 individual pins on the opposite side (**Fig. 1**). The pins fit into the wells of a 384-well plate, allowing the transfer of thermal energy between the metal plate and the liquid in each sample well. Excess thermal energy is dissipated from the opposite side of the thermoelectric modules by a hollow aluminum heat/cold sink in thermal contact with the thermoelectric modules. The temperature of the heat/cold sink was maintained by water circulation from a temperature-stable pump (F-12, Julabo). All thermoelectric modules were controlled by a PID controller (5C7-362, McShane) and were electrically supplied via a power supply (PS-24-20, TeTechnology). The instantaneous temperature values for controller feedback were obtained from a thermistor (TS67-170, McShane) buried in the metal plate. The PID controller was controlled via an interface with a PC and Mc362 software (McShane). The actual temperature readout that was relevant for measurements was carried out optically, through the amplitude of the fluorescent signal of the linearly temperature-sensitive dye[36] $[Ru(bpy)_3]^{2+}$ (Sigma) in multiple sample wells (50 µl at 100 µM). The temperature during any given time point was calculated by extrapolating start and end values of a temperature ramp. Ramp speeds of 2 °C s^{-1} and accuracies of ±0.1 °C and plate temperature homogeneity of <0.5 °C were achieved.

Screen. Transfected cells in 384-well plates were challenged with a temperature step from 25 to 42 °C for 120 s (**Fig. 1**). A final concentration of 25 µM 2APB was added on the same plates to determine the sensitivity of the clones to 2APB. Separate plates were prepared for stimulation by the addition of camphor to a final concentration of 1.75 mM. Concentration-response curves were obtained from three wells for a given compound concentration.

FLIPR data analysis. Screening data were analyzed with IGOR Pro (Wavemetrics). Raw data were pooled from all plates. We calculated maximal counts after individual baseline subtraction. Time curves for compound activation were fitted for each well by a mono-exponential function to obtain rate values. Histograms of maximal activations, their ratios and the rates of signal increases were produced for all mutants, wild-type TRPV3 controls ($n = 580$) and pcDNA controls ($n = 580$) (**Supplementary Fig. 1**). Histograms of controls were fitted with Gaussian distributions to obtain averages and standard deviations, which were used to calculate cut-off values for hit selection. We compared the maximal responses to each stimulus, their respective ratios and the signal rise times. In a primary screen, clones were considered to be hits that fulfilled all cut-off criteria for three or four wells. For the hit validation, 139 clones were regrown and re-analyzed using a similar, but more comprehensive, assay (16 wells for heat activation and 8 wells for each 2APB and camphor concentration). Cut-off values for hit confirmation were obtained by calculating the average values and s.d. of pooled data from positive (wild-type TRPV3) and negative (pcDNA) controls ($n = 240$ each) from all plates. We validated 44 clones as hits and sequenced their DNA. Full 2APB and camphor dose-response curves were measured for these clones and 15 were found to be identical to wild-type TRPV3 chemical responses. For concentration-response curves, maximal responses were calculated after baseline subtraction. Averages and s.d. were calculated from three wells, responses normalized to unity and fitted by a Hill equation.

Mutagenesis. All site-directed mutants were generated by QuikChange II XL Site-Directed Mutagenesis Kit (Stratagene). Domain swapping between mTRPV3 and other TRP channels was carried out using overlapping PCR and the QuikChange II XL Site-Directed Mutagenesis Kit, and all clones were verified by DNA sequencing. To generate mutant libraries containing 45 random point mutations for each amino acid between Leu642 and Thr660 of mouse TRPV3 and between E638 and P643 of *Xenopus* TRPV3, we designed primers that randomized the three nucleotides coding each amino acid (NNN) flanked by nucleotides that correctly encoded other amino acids adjacent to this specific position.

Electrophysiology. HEK293 cells were grown in DMEM containing 4.5 mg ml^{-1} glucose, 10% heat-inactivated fetal bovine serum, 50 units ml^{-1} penicillin and 50 µg ml^{-1} streptomycin. For patch-clamp recording, cells were co-transfected with enhanced green fluorescent protein and wild-type or mutant mTRPV3 constructs in 24-well plates using Fugene 6.0 (Roche), following the protocol provided by the manufacturer. Transfected HEK293 cells were reseeded on 12-mm round glass coverslips (Warner Instruments) 1 d after transfection. Whole-cell recordings were carried out the following day. Recording pipettes were pulled from micropipette glass (Sutter) to 2–4 MΩ when filled with a pipette solution containing 140 mM CsCl, 0.6 mM $MgCl_2$, 10 mM BAPTA and 10 mM Hepes, pH 7.20, and placed in a bath solution containing 140 mM NaCl, 5 mM KCl, 2 mM $CaCl_2$, 1 mM $MgCl_2$, 10 mM glucose and 10 mM Hepes, pH 7.4. Isolated cells were voltage clamped in the whole-cell mode using an EPC9 (HEKA Instruments) amplifier.

Voltage commands were made from the Pulse and PulseFit program and the currents were recorded at 5 kHz. Voltage ramps of 100 ms to +100 mV after a brief (20 ms) step to –100 mV from the holding potential of 0 mV were applied every second. Cells were continuously perfused with the bath solution through a Valve-Bank perfusion system (Automate Scientific). For current-voltage relationships, steady-state currents at the end of each voltage step were fitted as a function of the applied potential with a Boltzmann-function to obtain the V_{half} for each individual patch.

For experiments addressing the temperature activation of TRPV3 in HEK293 cells, the solution was heated using a CL-100 temperature controller (Warner Instruments) and an SC-20 Solution In-Line Heater/Cooler (Harvard Apparatus). Temperature was recorded with a thermistor placed <0.5 mm from the cell. Stock solutions of 2APB and camphor were made in DMSO. Whole-cell experiments were carried out at 25 °C.

The relative ion permeability, P, was calculated by shifts of reversal potentials ΔV after replacement of Na^+ by K^+, Cs^+, $NMDG^+$ or Ca^{2+} in the external buffer and the presence of 25 μM 2APB using the following equations:

$$\frac{P_X}{P_{Na}} = \left(\frac{[Na]}{[X]}\right) \cdot \exp\left(\frac{\Delta VF}{RT}\right) \quad (1)$$

$$\frac{P_{Ca}}{P_{Na}} = \left(\frac{[Na]}{4[Ca]}\right) \cdot \exp\left(\frac{\Delta VF}{RT}\right) \cdot \left(1 + \exp\left(\frac{FV_{Ca}}{RT}\right)\right) \quad (2)$$

[X] is the concentration of the given ion, F is Faraday's constant, R is the gas constant, T is the absolute temperature and V is the reversal potential for the replaced ion. For inside-out patches, both the pipette solution and bath solution contained 140 mM CsCl, 1 mM EGTA, 1 mM $MgCl_2$ and 10 mM Hepes, pH 7.4. The excised patches were held constantly at desired potentials while 2APB was repetitively applied and washed away from the bath through perfusion. Single-channel currents were recorded at 10 kHz and filtered at 3 kHz.

Molecular modeling. The mouse TRPV3 homology model was built using Prime 1.6 software from FirstDiscovery suite (Prime 1.6, Schrodinger) and Kv1.2 (Protein Database accession number 2A79) as a template. The structures were solvated in a truncated octahedron box consisting of TIP3P water molecules, where the distance between O and H atoms is 0.9752 Å, and the HOH angle is 104.52°, and periodic boundary conditions were applied[37]. The solvated complexes were subject to minimization, followed by 20 ps of constant volume and a subsequent 100 ps of constant pressure molecular dynamics equilibration runs at 300 K.

Cloning of *Xenopus tropicalis* TRPV3. Early juvenile *Xenopus tropicalis* were purchased from *Xenopus*One (Dexter). Total RNA was extracted from the whole brain of a frog using Trizol following the manufacturer's protocol (Invitrogen). First strand cDNA was prepared from the total RNA using SuperScript II reverse transcriptase (Invitrogen). PCR was carried out using the sense primer 5′-ATG TTA ACT GAT CTC CTT TCA GAA GCA AAG TCC AGT TCA AGG G-3′ and the antisense primer 5′-TTA CAT ACC AGG AAA AAA TGT TAA CCC AGG C-3′, which were designed to amplify putative full-length *Xenopus tropicalis* TRPV3 sequences (http://genome.jgi-psf.org/Xentr3/Xentr3.home.html/). The PCR product was cloned into a pCR2.1-TOPO vector (Invitrogen) and subcloned into the pcDNA5-FRT vector using *Kpn*I/*Not*I sites. Transient transfection of *Xenopus tropicalis* TRPV3 into HEK293 cells failed to give any responses to 2APB, camphor or heat (from 25 to 42 °C), probably because of missing N- and C-terminal sequences (predicted frog TRPV3 is considerably shorter than mammalian TRPV3s). To obtain a functional *Xenopus* TRPV3 channel, we added 134 amino acids (position 1 to 134) of mouse TRPV3 to the N terminus of the *Xenopus* TRPV3 downstream of the predicted methionine by overlap PCR. Similarly, 37 amino acids of mouse TRPV3 C terminus (position 755–791) were added to the end of *Xenopus* TRPV3 (with deletion of the last seven predicted amino acids of *Xenopus* TRPV3).

Note: Supplementary information is available on the Nature Neuroscience website.

ACKNOWLEDGMENTS

We thank A.J. Wilson and J. Mainquist for manufacturing the temperature device, A. Marelli and T. Orth for preparing miniprep DNA and M. Caterina for providing rat TRPV1 plasmid DNA. We thank T. Bartfai, E. Lattman, I. MacRae and A. Dubin for helpful discussion. This research was supported by grants from the US National Institutes of Health and by the Novartis Research Foundation.

AUTHOR CONTRIBUTIONS

J.G. and H.H. contributed equally to this work. J.G. and H.H. designed the study, collected and analyzed data and wrote the manuscript. M.B. participated in designing the temperature device. B.B. conducted molecular modeling. M.S. carried out the biochemical experiments. M.P. participated in producing the random mutant library. A.P. designed the study and wrote the manuscript. All authors discussed results and commented on the manuscript.

Published online at http://www.nature.com/natureneuroscience/
Reprints and permissions information is available online at http://npg.nature.com/reprintsandpermissions/

1. Dhaka, A., Viswanath, V. & Patapoutian, A. TRP ion channels and temperature sensation. *Annu. Rev. Neurosci.* **29**, 135–161 (2006).
2. Caterina, M.J. Transient receptor potential ion channels as participants in thermosensation and thermoregulation. *Am. J. Physiol. Regul. Integr. Comp. Physiol.* **292**, R64–R76 (2007).
3. Caterina, M.J. *et al.* The capsaicin receptor: a heat-activated ion channel in the pain pathway. *Nature* **389**, 816–824 (1997).
4. Guler, A.D. *et al.* Heat-evoked activation of the ion channel, TRPV4. *J. Neurosci.* **22**, 6408–6414 (2002).
5. Peier, A.M. *et al.* A heat-sensitive TRP channel expressed in keratinocytes. *Science* **296**, 2046–2049 (2002).
6. Xu, H. *et al.* TRPV3 is a calcium-permeable temperature-sensitive cation channel. *Nature* **418**, 181–186 (2002).
7. Watanabe, H. *et al.* Activation of TRPV4 channels (hVRL-2/mTRP12) by phorbol derivatives. *J. Biol. Chem.* **277**, 13569–13577 (2002).
8. Smith, G.D. *et al.* TRPV3 is a temperature-sensitive vanilloid receptor-like protein. *Nature* **418**, 186–190 (2002).
9. Neeper, M.P. *et al.* Activation properties of heterologously expressed mammalian TRPV2: evidence for species dependence. *J. Biol. Chem.* **282**, 15894–15902 (2007).
10. McKemy, D.D., Neuhausser, W.M. & Julius, D. Identification of a cold receptor reveals a general role for TRP channels in thermosensation. *Nature* **416**, 52–58 (2002).
11. Peier, A.M. *et al.* A TRP channel that senses cold stimuli and menthol. *Cell* **108**, 705–715 (2002).
12. Story, G.M. *et al.* ANKTM1, a TRP-like channel expressed in nociceptive neurons, is activated by cold temperatures. *Cell* **112**, 819–829 (2003).
13. Kobayashi, K. *et al.* Distinct expression of TRPM8, TRPA1 and TRPV1 mRNAs in rat primary afferent neurons with adelta/c-fibers and colocalization with trk receptors. *J. Comp. Neurol.* **493**, 596–606 (2005).
14. Moqrich, A. *et al.* Impaired thermosensation in mice lacking TRPV3, a heat and camphor sensor in the skin. *Science* **307**, 1468–1472 (2005).
15. Hu, H.Z. *et al.* 2-aminoethoxydiphenyl borate is a common activator of TRPV1, TRPV2, and TRPV3. *J. Biol. Chem.* **279**, 35741–35748 (2004).
16. Vogt-Eisele, A.K. *et al.* Monoterpenoid agonists of TRPV3. *Br. J. Pharmacol.* **151**, 530–540 (2007).
17. Xu, H., Blair, N.T. & Clapham, D.E. Camphor activates and strongly desensitizes the transient receptor potential vanilloid subtype 1 channel in a vanilloid-independent mechanism. *J. Neurosci.* **25**, 8924–8937 (2005).
18. Owsianik, G., D'Hoedt, D., Voets, T. & Nilius, B. Structure-function relationship of the TRP channel superfamily. *Rev. Physiol. Biochem. Pharmacol.* **156**, 61–90 (2006).
19. Owsianik, G., Talavera, K., Voets, T. & Nilius, B. Permeation and selectivity of TRP channels. *Annu. Rev. Physiol.* **68**, 685–717 (2006).
20. Bandell, M., Macpherson, L.J. & Patapoutian, A. From chills to chilis: mechanisms for thermosensation and chemesthesis via thermoTRPs. *Curr. Opin. Neurobiol.* **17**, 490–497 (2007).
21. Nilius, B. *et al.* Gating of TRP channels: a voltage connection? *J. Physiol. (Lond.)* **567**, 35–44 (2005).
22. Voets, T. *et al.* The principle of temperature-dependent gating in cold- and heat-sensitive TRP channels. *Nature* **430**, 748–754 (2004).
23. Voets, T. *et al.* TRPM8 voltage sensor mutants reveal a mechanism for integrating thermal and chemical stimuli. *Nat. Chem. Biol.* **3**, 174–182 (2007).
24. Brauchi, S., Orio, P. & Latorre, R. Clues to understanding cold sensation: thermodynamics and electrophysiological analysis of the cold receptor TRPM8. *Proc. Natl. Acad. Sci. USA* **101**, 15494–15499 (2004).
25. Latorre, R. *et al.* ThermoTRP channels as modular proteins with allosteric gating. *Cell Calcium* **42**, 427–438 (2007).
26. Matta, J.A. & Ahern, G.P. Voltage is a partial activator of thermo-sensitive TRP channels. *J. Physiol.* **585**, 469–482 (2007).
27. Brauchi, S. *et al.* Dissection of the components for PIP2 activation and thermosensation in TRP channels. *Proc. Natl. Acad. Sci. USA* **104**, 10246–10251 (2007).
28. Brauchi, S. *et al.* A hot-sensing cold receptor: C-terminal domain determines thermosensation in transient receptor potential channels. *J. Neurosci.* **26**, 4835–4840 (2006).
29. Bandell, M. *et al.* High-throughput random mutagenesis screen reveals TRPM8 residues specifically required for activation by menthol. *Nat. Neurosci.* **9**, 493–500 (2006).
30. Chung, M.K. *et al.* 2-aminoethoxydiphenyl borate activates and sensitizes the heat-gated ion channel TRPV3. *J. Neurosci.* **24**, 5177–5182 (2004).
31. Chung, M.K., Guler, A.D. & Caterina, M. Biphasic currents evoked by chemical or thermal activation of the heat-gated ion channel, TRPV3. *J. Biol. Chem.* **280**, 15928–15941 (2005).
32. Long, S.B., Campbell, E.B. & MacKinnon, R. Crystal structure of a mammalian voltage-dependent Shaker family K^+ channel. *Science* **309**, 897–903 (2005).
33. Jordt, S.E. *et al.* Acid potentiation of the capsaicin receptor determined by a key extracellular site. *Proc. Natl. Acad. Sci. USA* **97**, 8134–8139 (2000).
34. Ryu, S. *et al.* Uncoupling proton activation of vanilloid receptor TRPV1. *J. Neurosci.* **27**, 12797–12807 (2007).
35. Myers, B.R., Bohlen, C.J. & Julius, D. A yeast genetic screen reveals a critical role for the pore helix domain in TRP channel gating. *Neuron* **58**, 362–373 (2008).
36. Filevich, O. & Etchenique, R. 1D and 2D temperature imaging with a fluorescent ruthenium complex. *Anal. Chem.* **78**, 7499–7503 (2006).
37. Jorgensen, W.L., Chandrasekhar, J., Madura, J.D., Impey, R.W. & Klein, M.L. Comparison of simple potential functions for simulating liquid water. *J. Chem. Phys.* **79**, 926–935 (1983).